Glitch style visualization of disrupted neuronal connectivity in Parkinson's disease

Tim McGraw*

Purdue University

ABSTRACT

Neuronal connectivity graphs can give valuable insight into the structure of the brain and patterns of functional activity. In this paper we describe a connectivity visualization technique using contrasting styles to emphasize the differences between pairs of graphs. Our proposed technique enables interactive exploration of connectivity graphs at the various levels of the hierarchical structure of the brain - atlas regions, brain lobes and cerebral hemispheres. We demonstrate our methods on data obtained from matched pairs of subjects in a Parkinson's disease (PD) study. Control group data is displayed in a smooth, organic style with continuous transitions between views at different levels of the brain hierarchy using edge bundling and a new *node bundling* technique. Data from the PD group is displayed with glitch and noise effects inspired by PD symptoms, highlighting the differences between each subject and their matched pair from the control group. We conclude by describing avenues for further evaluation of this preliminary work.

Keywords: glitch, graph visualization, neuronal connectivity, neuroimaging

1 INTRODUCTION

Node-link diagrams are commonly used to visualize graphs which may represent, for example, transport networks, social relations and gene ontology. But even graphs of a moderate size can result in an unreadable "hairball" visualization, such as in Figure 1, right. In this work we describe contrasting visualization techniques for comparing neuronal connectivity graphs which reduce visual clutter using edge and node bundling, and emphasize areas of impaired connectivity with glitch art effects.

The central nervous system (CNS) is an interconnected network of cells with structural features at a range of spatial scales. Visualizing this network and understanding its features is a critical part of investigating the processes and diseases of the brain. Several imaging modalities can be used to assess neuronal connectivity at its various scales, including functional MRI (fMRI) [5], array tomography [26] and diffusion-weighted MRI (DWI) [8]. Reconstructing a complete map of the human "connectome", the set of all neuronal connections in the brain [35], is expected to lead to advances in diagnosis and treatment of many disorders, such as Parkinson's disease.

In this work we address the problem of visualizing macroscale structural connectivity graphs computed from DWI, and demonstrate our methods on data from a Parkinson's disease study. We use edge and node bundling to present a clean, smooth and uncluttered view of control group subjects to the user. By continuously transitioning between views at different levels of the brain hierarchy, we allow the user to maintain visual context of the parent-child relationships implicit in the data. Similar to the way in which edge bundling techniques can bend and merge together similar edges, our node bundling method can continuously group together related nodes in the graph by using a hybrid graphical representation: parametric curves for the edges and implicit curves for the nodes. Differences between datasets are emphasized using visual effects inspired by glitch art and which are evocative of Parkinson's disease (PD) symptoms, in order to draw attention to local areas of impaired connectivity.

*e-mail: tmcgraw@purdue.edu

2 BACKGROUND

In this section we present an overview of related work, including connectivity computation, graph visualization, Parkinson's disease, and the glitch art style that inspired our visual design.

2.1 Connectivity mapping

DWI has been used, quite effectively, to assess macroscale structural connectivity in the brain. We cannot provide a complete overview here, but Pfister et al. [29] and Margulies et al. [21] provide introductions to the imaging process and surveys of the related visualization literature. Tractography [4] – the process of reconstructing white matter fiber pathways – forms the basis of many connectivity mapping algorithms. However, visualizing whole brain connectivity by displaying all possible fiber tracts is impractical due to the large number of fibers and the occlusion of interior fibers by cortical fibers near the surface of the brain. Instead, connectivity can be quantified statistically based on the number of fibers that connect one region to another. Scalar field visualization can be used to display connectivity from a single region to all others. A volume rendered connectivity map [24, 23] using this approach is shown in Figure 1.

The work described in this paper is an extension of our previous work on GPU-based connectivity mapping [24, 23] and connectivity graph visualization [22]. As in [23] we compute a connectivity matrix, $C_{i,j}$, on the GPU based from 4th-order fiber orientation tensors [37] computed from high angular resolution DWI. The row and column indices of $C_{i,j}$ correspond to anatomical regions defined by the automated anatomical labeling (AAL) brain atlas [36] which consists of 116 gray matter structures. A slice of the atlas is shown in Figure 4. We have further grouped the 116 regions into brain lobes (shown in Table 1) and brain hemispheres (left, right, bilateral) to define a hierarchical structure. The connectivity matrix can be interpreted as the adjacency matrix which defines a connectivity graph. A spatial embedding of the graph is determined by positioning nodes at the centroid of their corresponding atlas regions. For the 2D visualizations presented in this paper, those node locations are projected onto one of the standard imaging planes.

2.2 Connectivity visualization

The structure of small connectivity graphs can sometimes be revealed by directly displaying the connectivity matrix as a colormapped image (see Figure 1, left). Many variations on this approach have been proposed [12, 33, 17], but the drawback shared by these methods is that the anatomical meaning of the nodes, as conveyed by position, is lost.

Node-link visualizations of graphs tend to suffer from visual clutter due to overlapping edges and nodes. This weakness can

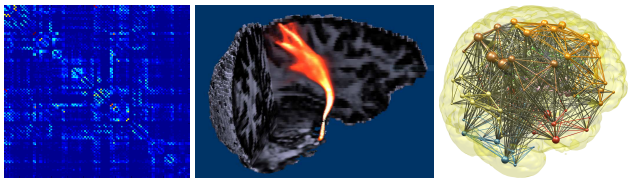

Figure 1: Connectivity matrix visualization(left), volume rendered connectivity (middle), and a 3D graph of neuronal connectivity (right). Even though there are only 116 nodes, the interior of the graph is severely occluded. Sources: [23], [22].

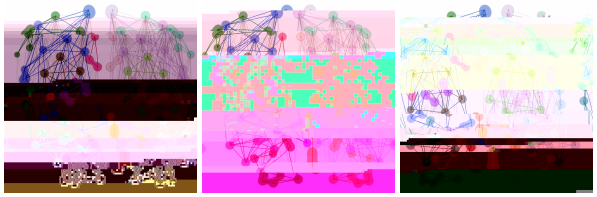

Figure 2: Glitched images of connectivity graphs obtained by changing bytes in a JPEG encoded image. Header information controlling the width, height and number of color components was left unchanged.

be addressed by using edge bundling [18] to cluster edges and steer them around nearby nodes. Previous approaches to 3D connectivity visualization have used this approach [6]. Others have instead used adjusted node positions, using e.g. a circular layout scheme [19] or a subway map metaphor [1]. However, these node layout schemes distort the spatial relations between nodes and the resulting visualization loses some of its anatomical meaning. A general approach to solving the problem of edge cluttering using node-ring diagrams was described by Etemad et al. [14]. Their approach eliminates edge drawing altogether and encodes connectivity using concentric rings of color.

Node aggregation techniques simplify a graph by allowing a single node to visually represent multiple nodes. The applications include scalable visualization of large graphs [38] and representing hierarchical relations [13]. Unlike previous approaches, our node bundling implementation maintains a discrete node-link appearance, rather than appearing as a heatmap [38], and allows us to display overlapping groups of aggregated nodes.

We previously [22] developed a 2D connectivity graph visualization approach which introduced a new edge bundling criterion based on anatomical compatibility, used a node layout based on AAL atlas region locations and performed additional visual clutter reduction by separating inter- and intrahemispheric displays. In this paper we extend those methods by adding

- glitch-style visualization techniques for emphasizing areas of abnormal connectivity, and
- a graphical technique for displaying hierarchical node aggregation which permits smooth continuous visualization during graph interaction.

2.3 Glitch art

The term 'glitch' was famously used by John Glenn to describe transient spikes in electrical voltage which led to spacecraft malfunctions [16]. Much glitch art is inspired by errors that can occur during transmission or storage of images. Whether intentional or not, missing data or noise in these processes leads to unexpected distortions of the resulting image [25]. Sometimes these artifacts are specific to certain file formats. For example, missing I-frames in MPEG videos, and modified Huffman tables in JPEG images lead to characteristic block and raster distortions due to the way compression is implemented. Experiments in this area can involve simply corrupting files in a hex or text editor [11], leading to unforeseen image distortions, as shown in Figure 2.

Other types of glitches can be implemented by generalizing from compression/decompression to other types of transformations in the spatial or color domain and introducing some modification between the forward/inverse transform steps [31].

In this work we explore a parallel between glitched images and the corruption of motor and sensory information in the brain due to Parkinson's disease. Image glitches are often characterized by a nonlinear relation between a small error and its resulting drastic visual effect. Analogously, minor disruptions in brain chemistry and electrical signaling can lead to major changes in sensory and motor function. Glitches in the graph visualization serve the practical purpose of emphasizing differences in connectivity between healthy control subjects and subjects suffering from Parkinson's disease.

2.4 Parkinson's disease

Parkinson's disease is progressive disorder of the CNS associated with impaired cognitive and motor function. There is no known cause or cure, but treatment can alleviate the symptoms. Onset is typically in middle age, and about 60,000 people in the US are diagnosed each year. It is estimated that more than 7 million people worldwide suffer from the disease [27]. A wide range of symptoms can occur, including rest tremor, bradykinesia (slowness of movement), and rigidity [20]. Changes in vision can include losses of visual acuity, contrast sensitivity, color discrimination, and motion perception [2]. Both increases [9] and decreases [34] in creativity and artistic expression have been reported.

The disease is commonly associated with frontal lobe dysfunction. Although anatomic T1- and T2-weighted MR images are usually normal in PD patients, changes in functional connectivity from fMRI [3] and structural connectivity from DWI [15] have been measured in PD patients.

3 Methods

In this section we describe the implementation of our visualization application which was developed in C++ and OpenGL. The input to our method is a pair of connectivity matrices computed using the methods described by McGraw [22]. Our results were generated using a publicly available dataset from the Neuroimaging Informatics Tools and Resources Clearinghouse (NITRC). The image data was acquired from 53 subjects in a cross-sectional Parkinson's disease (PD) study. The dataset contains diffusion-weighted images of 27 PD patients and 26 age, sex, and education-matched control subjects. The matched pairs experimental design explicitly controls for differences in subject attributes, such as sex and age which can have an effect on neuronal connectivity. This design permits an analysis of differences between matched pairs of subjects, rather than the differences of the averages of groups. The latter approach can average out differences between individuals and permit outliers to unduly influence the analysis.

The dataset for each subject consists of 120 diffusion-weighted images with diffusion weighting factors b=1000 and b=2500 s/mm^2, and isotropic 2.4 mm^3 voxels. The imaging protocol used a twice-refocused spin echo sequence in order to avoid distortions induced by eddy currents. The data were postprocessed to reduce motion artifacts.

After computing the connectivity matrix, C, for each subject, the mean and variance of connectivity values for subjects in each group (PD and control) were computed. A node-link diagram of the resulting intrahemispheric connectivity graph of 904 edges without edge bundling is shown in Figure 3. There is one node per AAL atlas region in the graph. Nodes belonging to the same lobe were

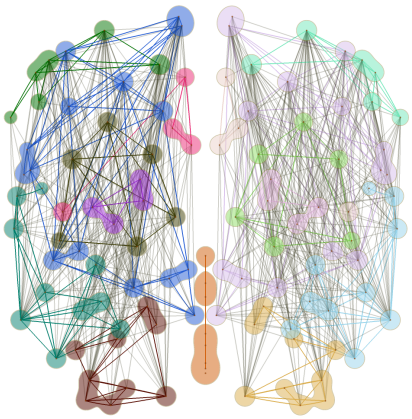

Figure 3: Control group intrahemispheric connectivity graph without edge bundling.

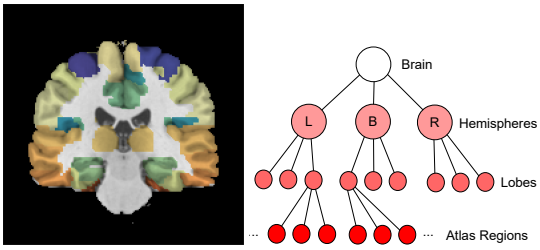

Figure 4: A coronal slice of T1-weighted MRI overlaid with color-coded AAL atlas regions (left), and hierarchical structure of the brain (right) from root to leaves: brain, hemisphere, lobe, region.

assigned the same color, and drawn as circles with radius proportional to node degree (the number of incident edges). The visual clutter apparent in this image due to overlapping edges will be reduced by edge bundling.

3.1 Node Bundling

In this work we extend the concept of edge bundling to the nodes of a graph. This technique permits nodes to smoothly blend and merge together for level-of-detail applications or to represent hierarchical relationships between nodes, such as the hemisphere-lobe-region relations shown in Figure 4. The different graphical representations of the nodes and edges require them to be rendered in separate passes with different shaders. Edges are rendered as line strips, and nodes are rendered as quadrilaterals or point sprites.

Node bundling requires two rendering passes, detailed below.

Pass 1: point sprite rendering. This pass is rendered to a floating-point texture, $f(x,y)$, while additive alpha blending is enabled. A single point sprite for each node is rendered. Each point sprite is procedurally textured in the fragment shader with a 2D Gaussian centered at the middle of the sprite.

Pass 2: isocontour rendering. A full-screen quadrilateral is rendered. In the fragment shader the isocontour is rendered by thresholding the texture. The node color is rendered where $f(x,y) > 0$, all other fragments are discarded.

In pass 1, when point sprites overlap, additive alpha blending causes nearby nodes to blend together, as in metaball modelling [32]. The final image of the graph nodes is an isocontour of a Gaussian mixture. When nodes are far enough apart two distinct contours will be seen, but as they become closer they will merge together into a single contour, as seen in Figure 6. The implementation of pass 1 is similar to the method described by Zinsmaier et al. [38], but our method maintains a discrete node appearance with a distinct boundary, and we combine nodes based on hierarchical relations, not only distance.

Figure 5: The aliasing issue (left) can be addressed by using a smooth thresholding function (middle). Computing a distance function estimate permits more precise control over the boundary width (right).

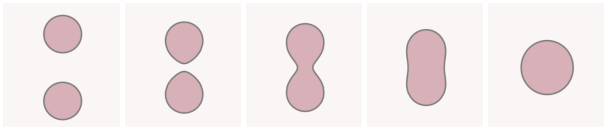

Figure 6: Node bundling : two graph nodes continuously merge together.

In our application, we use an anatomical node bundling criterion - only nodes in the same brain lobe should be bundled together. Note in Figure 3 that nodes in the same lobe (which have the same color) bundle together when they are nearby, but remain separate from, and can even overlap nodes in a different lobe. In order to achieve this, the nodes of each lobe must be rendered to a separate floating-point texture. This requires a total of two render passes per lobe, but the OpenGL layered rendering feature greatly reduces this number by permitting fragments to be directed to a specific framebuffer attached texture. Using the definitions in Table 1 and accounting for the left-right pairs of lobes (except Central Structures) we require a total of 13 texture attachments to prevent nodes from different lobes from interfering with each other.

Simple thresholding of the texture values in pass 2 causes aliasing, so we use a sigmoid function to soften the boundaries of the nodes. A pair of sigmoid functions can be used to create an outline for each node, but the naïve implementation will lead to variable width lines. To overcome this artifact we compute from the texture image, denoted as $f(x,y)$, a first order estimate of a signed distance function,

$$d(x,y) \approx \frac{f(x,y)}{||\nabla f(x,y)||}. \quad (1)$$

The gradient can be estimated using the glsl screen-space derivative functions dFdx() and dFdy(), but precision issues leave some artifacts in the results. Instead, we compute the gradient using central differences in the fragment shader. The effects of applying soft thresholding and distance estimation to $d(x,y)$ are shown in Figure 5. The appearance of multiple nodes as they continuously merge together is shown in Figure 6.

Our application supports interactive selection of lobes and regions. Initially, the atlas regions (the lowest level of the brain hierarchy described by Figure 4) are shown. Selection of an anatomical region with the mouse triggers the collapse of all regions belonging to the same lobe as the selected region. This corresponds to visualizing connectivity at a higher hierarchical level. During collapse, intraregion edges are faded out. Clicking a collapsed lobe triggers expansion of the regions back to their original locations. See the supplementary video for a demonstration of node bundling.

Temporal Lobe	Hippocampus, Parahippocampus, Amygdala, Fusiform gyrus, Heschl gyrus, Superior temporal gyrus, Temporal pole: superior temporal gyrus, Middle temporal gyrus, Temporal pole: middle temporal gyrus, Inferior temporal gyrus
Posterior Fossa	Cerebellum, Vermis, Medulla, Midbrain, Pons
Insula and Cingulate Gyri	Insula, Cingulate gyrus (ant., mid, post.)
Frontal Lobe	Precentral gyrus, Superior frontal gyrus, Middle frontal gyrus, Inferior frontal gyrus, Rolandic operculum, Supplementary motor area, Olfactory cortex, Gyrus rectus, Paracentral lobule
Occipital Lobe	Calcarine fissure and surrounding cortex, Cuneus, Lingual gyrus, Occipital lobe (sup., mid. and inf.)
Parietal Lobe	Postcentral gyrus, Superior parietal gyrus,Inferior parietal gyrus, Supramarginal gyrus, Angular gyrus, Precuneus
Central Structures	Caudate nucleus, Putamen, Pallidum, Thalamus

Table 1: Lobes of the brain and the AAL regions which comprise them. All lobes, except for Central Structures, consist of left-right pairs.

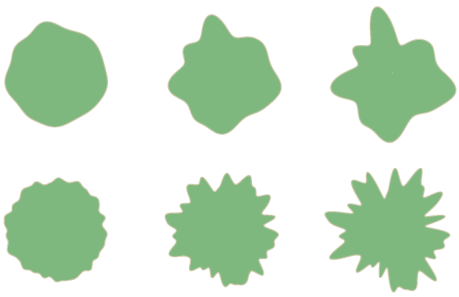

Figure 7: Node glitch effects. Noise amplitude increases from left to right. Low frequency noise added (top row), high frequency noise added (bottom row).

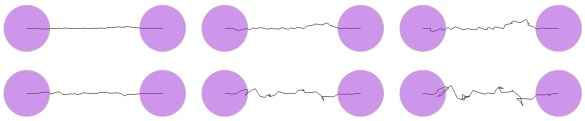

Figure 8: Edge glitch effects. Noise amplitude increases from left to right. Low frequency noise added (top row), high frequency noise added (bottom row). High spatial frequencies result in more self-intersections.

3.2 Glitch Visualization Style

Connectivity graphs visualized using edge and node bundling have a smooth and organic visual style. This is the approach we use for displaying connectivity of the control subjects. We display PD datasets in a glitch style reflecting typical PD symptoms, such as tremor and visual disturbances. The glitch effects we incorporate into the visualization include

- Desaturated colors, reflecting the loss of color contrast sensitivity in PD patients
- Jagged edges, reflecting the appearance of lines drawn by someone suffering from tremor
- Noisy displacement added to the node shape
- Video-style glitch effects of color-separation and block noise added in image-space.

We avoided using actual JPEG glitches, such as those in Figure 2 since those effects can severely alter the spatial relations between nodes in the graph, and sometimes make large parts of the image unreadable due to the appearance of large blocks with low contrast.

Node glitches. The smooth circular shapes of nodes are displaced by noise having amplitude proportional to the absolute difference in node degree compared to the corresponding node in the control data. Since we use an implicit representation of the node shape to permit node bundling it is quite simple to distort the shape of the boundary. Perlin noise [28] is added directly to the Gaussian function generated in pass 1 of node rendering. Examples of the displacement effect are shown in Figure 7. We experimented with using varying spatial frequencies of noise to indicate increase or decrease in node degree, but relative frequencies proved difficult to read in a full graph visualization.

Edge glitches. Edges between nodes have 2 octaves of Perlin noise added, mimicking the effects of lines drawn by Parkinson's patients. Such lines can be found in the PD literature regarding 'spiral analysis', a test used to assess severity of motor symptoms [30] by analyzing the drawings produced by patients asked to reproduce an Archimedes spiral. Similar noisy edges have previously been used as a metaphor for uncertainty in graph drawing [7]. Sample edge glitches are shown in Figure 8. As with the node displacement glitch, it is possible to map the noise frequency to some property, but in our final results we use only a single frequency. For each edge the amount of noise added was proportional to the edge connectivity difference between the Parkinson's subject and the matched control subject.

The noisy edge displacement is also motivated by a glitch we observed in the physics simulation which governs the edge bundling computation. Too high of a timestep can lead to numerical instability which manifests as jagged edges. However, this instability can lead to edges being totally displaced from the image, so we decided not to use this instability to implement the glitch. Instead, we fake the glitch by adding noise in the vertex shader. We use the same edge bundling technique as described in [22], but in our application bundling is performed in an OpenGL compute shader to maintain an interactive frame rate. Since the glitch is applied in the vertex shader, the edge bundling performed in the compute shader is not affected by the added noise.

Lobe glitches. Color field and scan line glitches corrupt the overall image of lobes, as shown in Figure 9. The glitches are applied in pass 2 of node rendering. Recall that all nodes in the same lobe are rendered into a single texture, so we can easily corrupt the image of an entire lobe in the fragment shader. The severity of the corruption is proportional to the overall intralobe connectivity difference between the PD subject and the matched control subject. Animation

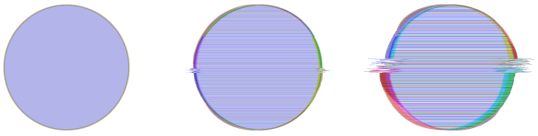

Figure 9: Lobe glitch effects. Glitch magnitude increases from left to right. The effects include distorted scan lines, color channel separation, and block noise.

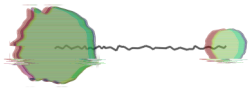

Figure 10: An example of a two node graph with glitch effects on nodes and edges.

of this effect (see supplementary files) has the timestep distorted by noise, which mirrors the effects of tremor and visual symptoms of altered motion perception.

The lobe glitch effects were inspired by the JPEG corruption effects, but were designed to only corrupt at a small scale and maintain readability of the graph. Alternating scanlines have some color components reduced in magnitude, but even at high glitch levels the overall hue of the nodes is not changed significantly. The color channels of the texture were displaced by a low frequency noise function to mimic a broken CRT. Higher frequency and amplitude displacement was applied to a small number of rows of the image to simulate signal transmission noise. Finally color saturation was boosted. Although Parkinson's visual symptoms may include loss of color sensitivity, we found that decreases in saturation were more difficult to perceive than increases.

A two node synthetic graph with a combination of node, edge and lobe glitch effects is shown in Figure 10.

Individual and group average connectivity graphs were processed and visualized. Statistical significance of average connectivity differences was determined by computing the average difference in connectivity matrices $\bar{C}_{\text{diff}} = \overline{C_{\text{PD}} - C_{\text{control}}}$. A paired two-sample t-test at the 5% confidence level was performed for each pair of nodes (i, j). If the test did not indicate that we should reject the null hypothesis (that the connectivity in the subjects is equal) then the edge between i and j was not drawn. Then $\bar{C}_{\text{diff}}$ was used in the shader when applying glitch effects to the PD average connectivity visualization.

For individual data, we compute the mean, $\bar{C}_{\text{control}}$, and standard deviation, S, of the control group connectivity values. Connectivity differences between PD and control greater than two standard deviations were emphasized with glitch effects.

4 Results

Parkinson's disease is associated with disrupted intrahemispheric neuronal connectivity, primarily in the frontal, temporal and parietal lobes [10]. Control group mean intralobe and interlobe connectivity graphs are shown in Figures 11 and 12. The statistically significant connectivity differences observed in the PD group is emphasized in those figures using glitch effects. These are most obvious in the frontal, parietal and temporal lobes. The graphs shown in this section were laid out in the coronal imaging plane. Note that the left-right hemisphere asymmetry obvious in the results presented here is expected. Possible causes include image noise, hard thresholding of values during connectivity matrix computations and lateralization of brain function. Functions such as speech and language are known to be controlled by the left cerebral hemisphere, especially the temporal and parietal lobes.

Though PD changes are primarily intrahemispheric, the edge bunding behavior is demonstrated on control group interhemispheric connectivity in Figure 13.

Connectivity visualization of a matched pair of subjects is shown Figure 14. Subject p07183 is a 59 year old male from the control group, and p06316 is a 60 year old male who has suffered from Parkinson's symptoms for 2 years. Large differences in connectivity within the frontal lobe are emphasized by the jagged edges and color separation glitches in the graph nodes. (Refer to Figure 12 for frontal lobe location and color.)

Another matched pair is shown Figure 15. Subject p07519 is a 63 year old male, and p06904 is a 62 year old male with disease duration of 13 years. The motor abilities of subjects p06316 and p06904 are most affected on the right side of the body, implicating the left hemisphere of the brain (shown on the right side of the figures by radiological convention). In both cases the glitch effects are most apparent on the right sides of the figures.

5 Conclusions and Future Work

In this exploratory work we have presented methods for glitch style graph visualization and interactive node bundling. Both techniques were demonstrated in the context of visualizing neuronal connectivity graphs computed from a Parkinson's disease study. The glitch effects we used to emphasize the differences between PD and control subjects were inspired by Parkinson's disease symptoms. Visual clutter in the graph visualization was reduced by using edge and node bundling. We demonstrated how the hierarchical structure of the brain (hemisphere, lobes and regions) can be explored interactively with continuous visual transitions between hierarchical levels (e.g. from individual atlas regions to lobes).

Our visualizations results reflect existing knowledge of frontal, parietal and temporal lobe connectivity changes associated with Parkinson's disease, but further evaluation is needed. We have identified several directions for future work to evaluate the preliminary results we have presented here, including user studies to assess (1) the impact of interactive node bundling on the understanding of hierarchical relations in graphs, (2) how glitch-style visualization affects the ability of experts to identify areas of impaired connectivity in connectivity graphs, and (3) if glitch effects help students and laypeople understand neuroanatomy and symptoms of neurological diseases.

Acknowledgements

The authors wish to thank NVIDIA Corporation for the donation of graphics hardware used in this project.

References

[1] A. Al-Awami, J. Beyer, H. Strobelt, N. Kasthuri, J. Lichtman, H. Pfister, and M. Hadwiger. Neurolines: A subway map metaphor for visualizing nanoscale neuronal connectivity. *IEEE Transactions on Visualization and Computer Graphics (Proceedings IEEE InfoVis 2014)*, 20(12):2369–2378, 2014.

[2] R. A. Armstrong. Visual symptoms in Parkinson's disease. *Parkinson's Disease*, 2011, 2011.

[3] H.-C. Baggio, R. Sala-Llonch, B. Segura, M.-J. Marti, F. Valldeoriola, Y. Compta, E. Tolosa, and C. Junqué. Functional brain networks and cognitive deficits in Parkinson's disease. *Human Brain Mapping*, 35(9):4620–4634, 2014.

[4] P. J. Basser, S. Pajevic, C. Pierpaoli, J. Duda, and A. Aldroubi. In vivo fiber tractography using DT-MRI data. *Magnetic Resonance in Medicine*, 44(4):625–632, 2000.

[5] T. E. Behrens and O. Sporns. Human connectomics. *Current Opinion in Neurobiology*, 22(1):144–153, 2012.

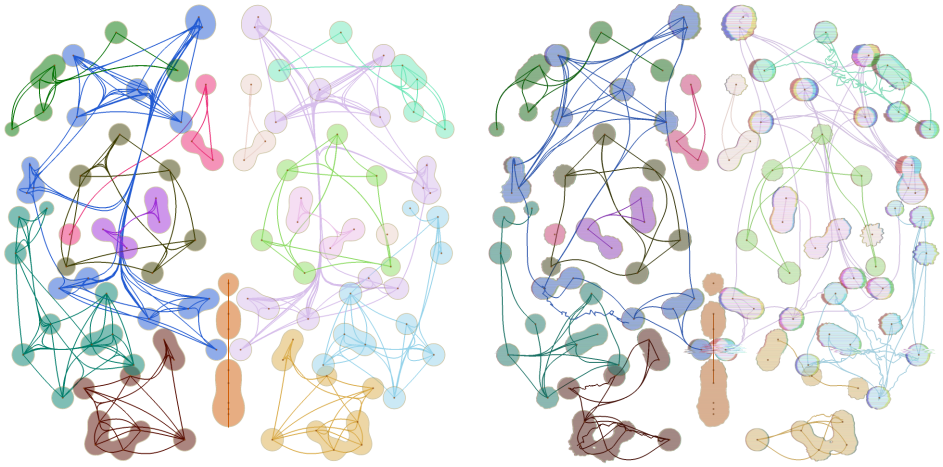

Figure 11: Control group (left) and PD group (right) mean intralobe connectivity graphs.

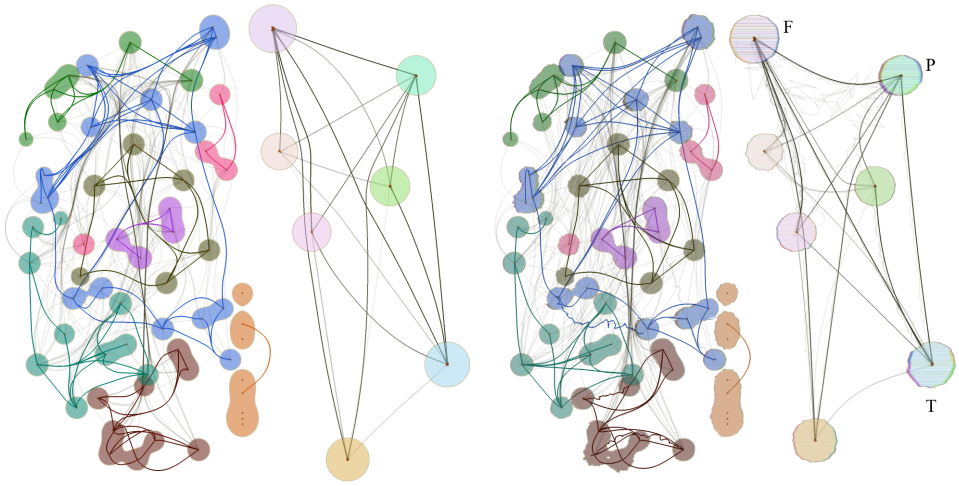

Figure 12: Control group (left) and PD group (right) mean connectivity graphs. Intralobe edges are colored, and interlobe edges are grey. In the left hemisphere the graph is collapsed to the lobe level of the hierarchy. Frontal, Parietal and Temporal lobes are annotated F, P and T, respectively.

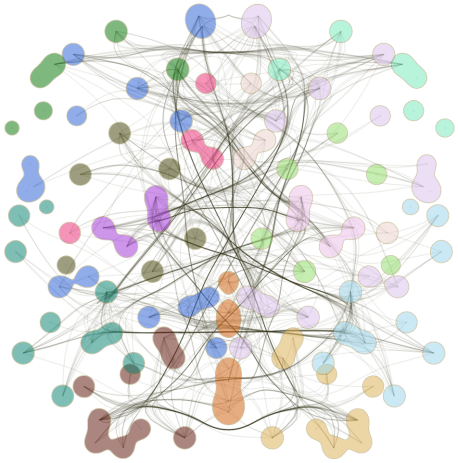

Figure 13: Control group mean interhemispheric connectivity graph.

[6] J. Bottger, A. Schafer, G. Lohmann, A. Villringer, and D. S. Margulies. Three-dimensional mean-shift edge bundling for the visualization of functional connectivity in the brain. *IEEE Transactions on Visualization and Computer Graphics*, 20(3):471–480, 2014.

[7] N. Boukhelifa, A. Bezerianos, T. Isenberg, and J.-D. Fekete. Evaluating sketchiness as a visual variable for the depiction of qualitative uncertainty. *IEEE Transactions on Visualization and Computer Graphics*, 18(12):2769–2778, 2012.

[8] L. Cammoun, X. Gigandet, D. Meskaldji, J. P. Thiran, O. Sporns, K. Q. Do, P. Maeder, R. Meuli, and P. Hagmann. Mapping the human connectome at multiple scales with diffusion spectrum MRI. *Journal of Neuroscience Methods*, 203(2):386–397, 2012.

[9] A. Chatterjee, R. H. Hamilton, and P. X. Amorapanth. Art produced by a patient with Parkinson's disease. *Behavioural Neurology*, 17(2):105–108, 2006.

[10] A. Cronin-Golomb. Parkinson's disease as a disconnection syndrome. *Neuropsychology review*, 20(2):191–208, 2010.

[11] E. den Heijer. *Evolving glitch art*. Springer, 2013.

[12] K. Dinkla, M. A. Westenberg, and J. J. van Wijk. Compressed adjacency matrices: Untangling gene regulatory networks. *IEEE Transactions on Visualization and Computer Graphics*, 18(12):2457–2466, 2012.

[13] N. Elmqvist and J.-D. Fekete. Hierarchical aggregation for information visualization: Overview, techniques, and design guidelines. *IEEE Transactions on Visualization and Computer Graphics*, 16(3):439–454, 2010.

[14] K. Etemad, S. Carpendale, and F. Samavati. Node-ring graph visualization clears edge congestion. *Proceedings of the IEEE VIS Arts Program (VISAP)*, pages 67–74, 2014.

[15] G. Gattellaro, L. Minati, M. Grisoli, C. Mariani, F. Carella, M. Osio, E. Ciceri, A. Albanese, and M. Bruzzone. White matter involvement in idiopathic Parkinson's disease: a diffusion tensor imaging study. *American Journal of Neuroradiology*, 30(6):1222–1226, 2009.

[16] J. Glenn. *Into Orbit*. Cassell, London, 1962.

[17] N. Henry, J.-D. Fekete, and M. J. McGuffin. Nodetrix: A hybrid visualization of social networks. *IEEE Transactions on Visualization and Computer Graphics*, 13(6):1302–1309, 2007.

[18] D. Holten and J. J. Van Wijk. Force-directed edge bundling for graph visualization. *Computer Graphics Forum*, 28(3):983–990, 2009.

[19] A. Irimia, M. C. Chambers, C. M. Torgerson, and J. D. Van Horn. Circular representation of human cortical networks for subject and population-level connectomic visualization. *NeuroImage*, 60(2):1340–1351, 2012.

[20] J. Jankovic. Parkinson's disease: clinical features and diagnosis. *Journal of Neurology, Neurosurgery & Psychiatry*, 79(4):368–376, 2008.

[21] D. S. Margulies, J. Böttger, A. Watanabe, and K. J. Gorgolewski. Visualizing the human connectome. *NeuroImage*, 80:445–461, 2013.

[22] T. McGraw. Graph-based visualization of neuronal connectivity using matrix block partitioning and edge bundling. In *Advances in Visual Computing*, pages 3–13. Springer, 2015.

[23] T. McGraw and D. Herring. High-order diffusion tensor connectivity mapping on the GPU. In *Advances in Visual Computing*, pages 396–405. Springer, 2014.

[24] T. McGraw and M. Nadar. Stochastic DT-MRI connectivity mapping on the GPU. *IEEE Transactions on Visualization and Computer Graphics*, 13(6):1504–1511, 2007.

[25] R. Menkman. Glitch studies manifesto. *Video vortex reader II: Moving images beyond YouTube*, pages 336–347, 2011.

[26] K. D. Micheva and S. J. Smith. Array tomography: A new tool for imaging the molecular architecture and ultrastructure of neural circuits. *Neuron*, 55(1):25–36, 2007.

[27] Parkinson's disease foundation - statistics on Parkinson's. `http://www.pdf.org/en/parkinson_statistics`. Accessed: 2016-05-29.

[28] K. Perlin. Improving noise. In *ACM Transactions on Graphics*, volume 21, pages 681–682. ACM, 2002.

[29] H. Pfister, V. Kaynig, C. P. Botha, S. Bruckner, V. J. Dercksen, H.-C. Hege, and J. B. Roerdink. Visualization in connectomics. In *Scientific Visualization*, pages 221–245. Springer, 2014.

[30] R. Saunders-Pullman, C. Derby, K. Stanley, A. Floyd, S. Bressman, R. B. Lipton, A. Deligtisch, L. Severt, Q. Yu, M. Kurtis, et al. Validity of spiral analysis in early parkinson's disease. *Movement disorders*, 23(4):531–537, 2008.

[31] T. Schachman. Tranforms, inverse transforms, and glitch. `http://pixelshaders.com/misc/glitch/`. Accessed: 2016-05-15.

[32] J. Shen and D. Thalmann. Interactive shape design using metaballs and splines. In *Proc. Implicit Surfaces '95*, 1995.

[33] Z. Sheny and K.-L. Maz. Path visualization for adjacency matrices. In *Proceedings of the 9th Joint Eurographics/IEEE VGTC conference on Visualization*, pages 83–90. Eurographics Association, 2007.

[34] H. Shimura, R. Tanaka, T. Urabe, S. Tanaka, and N. Hattori. Art and Parkinson's disease: a dramatic change in an artists style as an initial symptom. *Journal of neurology*, 259(5):879–881, 2012.

[35] O. Sporns, G. Tononi, and R. Kötter. The human connectome: A structural description of the human brain. *PLoS Computational Biology*, 1(4):e42, 2005.

[36] N. Tzourio-Mazoyer, B. Landeau, D. Papathanassiou, F. Crivello, O. Etard, N. Delcroix, B. Mazoyer, and M. Joliot. Automated anatomical labeling of activations in SPM using a macroscopic anatomical parcellation of the MNI MRI single-subject brain. *NeuroImage*, 15(1):273–289, 2002.

[37] Y. T. Weldeselassie, A. Barmpoutis, and M. Stella Atkins. Symmetric positive semi-definite Cartesian tensor fiber orientation distributions (CT-FOD). *Medical Image Analysis*, 16(6):1121–1129, 2012.

[38] M. Zinsmaier, U. Brandes, O. Deussen, and H. Strobelt. Interactive level-of-detail rendering of large graphs. *IEEE Transactions on Visualization and Computer Graphics*, 18(12):2486–2495, 2012.

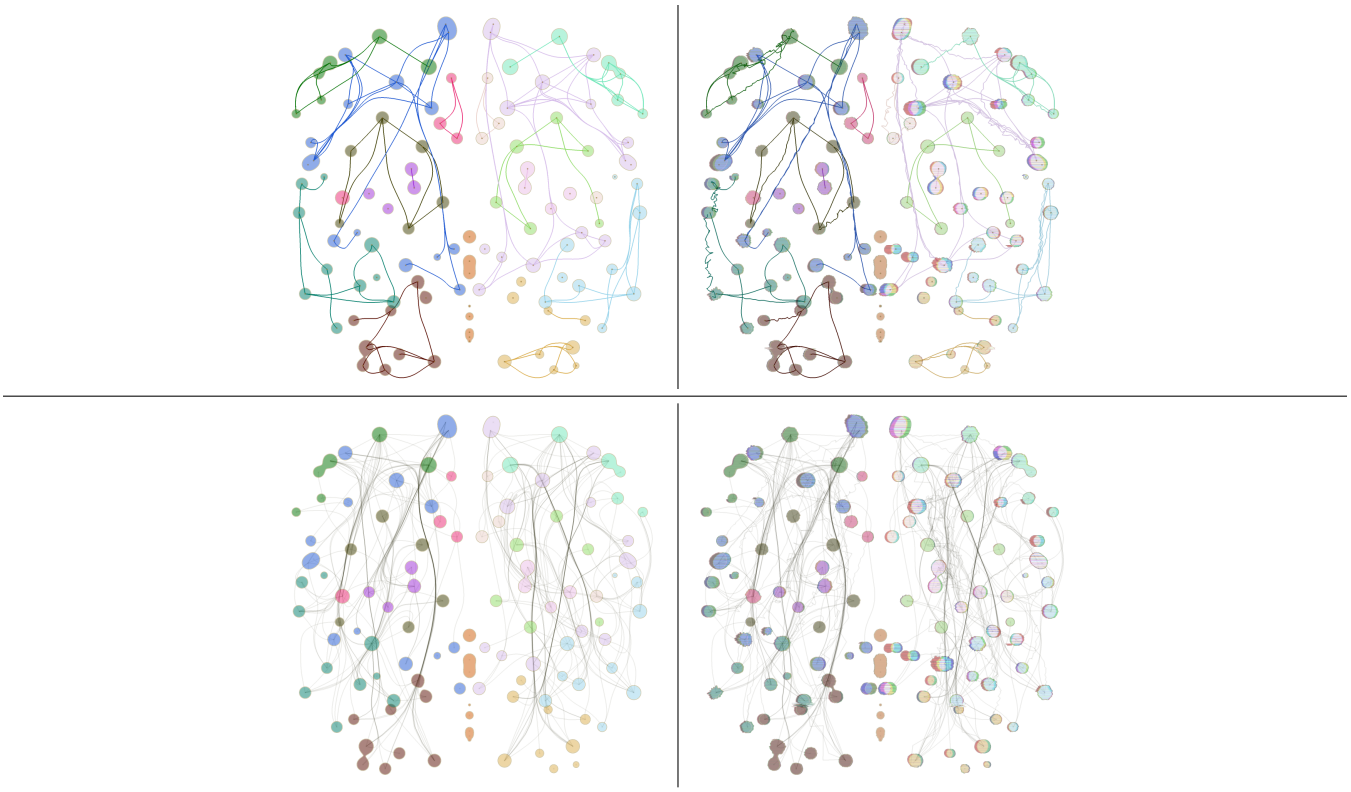

Figure 14: Control subject p07183 (left) and PD subject p06316 (right) intralobe (top) and interlobe (bottom) connectivity graphs.

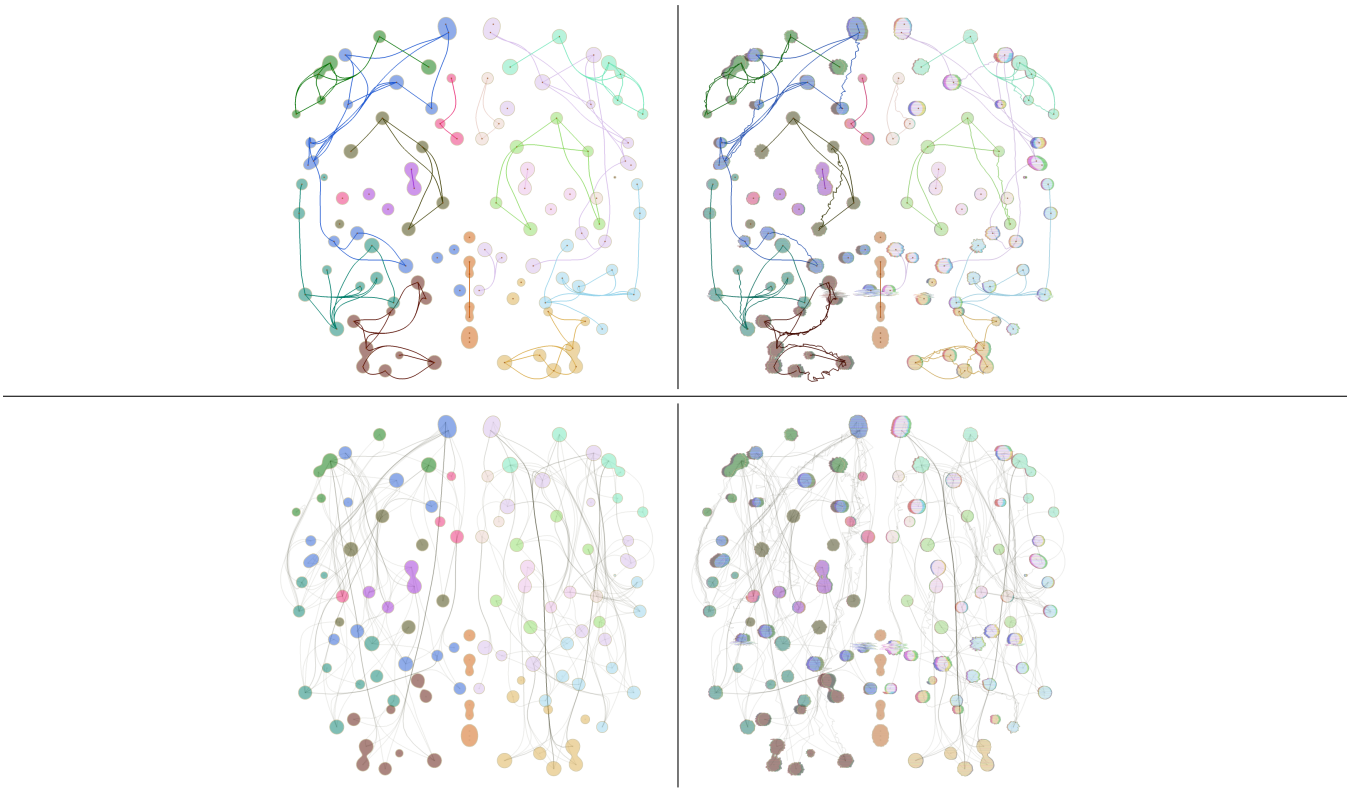

Figure 15: Control subject p07519 (left) and PD subject p06904 (right) intralobe (top) and interlobe (bottom) connectivity graphs.